

Coherent oscillations in a superconducting multi-level quantum system

J. Claudon¹, F. Balestro^{1,2}, F. W. J. Hekking³, and O. Buisson¹

¹*Centre de Recherches sur les Très Basses Températures,
laboratoire associé à l'Université Joseph Fourier,
C.N.R.S., BP 166, 38042 Grenoble-cedex 9, France*

²*Department of Nanoscience, Delft University of Technology,
Lorentzweg 1, 2628 CJ Delft, The Netherlands*

³*Laboratoire de Physique et Modélisation des Milieux Condensés,
CNRS & Université Joseph Fourier,
BP 166, 38042 Grenoble-cedex 9, France*

Abstract

We have observed coherent time evolution of states in a multi-level quantum system, formed by a current-biased dc SQUID. The manipulation of the quantum states is achieved by resonant microwave pulses of flux. The number of quantum states participating in the coherent oscillations increases with increasing microwave power. Quantum measurement is performed by a nanosecond flux pulse which projects the final state onto one of two different voltage states of the dc SQUID, which can be read out.

PACS numbers: 03.67.Lx, 05.45.-a, 85.25.-j

Up to now, in view of quantum information processing, experiments in solid state devices have concentrated only on the implementation of two-level quantum systems. A variety of quantum circuits based on Josephson junctions [1, 2, 3, 4, 5, 6, 7] and quantum dots [8, 9] have been proposed and realized. Rabi oscillations have been observed showing that the two lowest levels can be manipulated coherently. However, the two-level system is not the only one useful for quantum computation. For instance, multi-level systems are of interest for solving database search problems using quantum algorithms [10], as was demonstrated with Rydberg atoms [11]. Recent theoretical proposals discuss the use of multilevel quantum systems in solid state devices for quantum information processing [12, 13]. In superconducting devices such as a current-biased Josephson junction [14, 15] or a rf SQUID [16] and in molecular magnets [17, 18, 19, 20], many experiments were performed demonstrating the multi-level quantum nature of these systems. However no experiments have been performed yet which show coherent manipulation. In this letter, we demonstrate the first manipulation of, and measurement on a multi-level solid state circuit, based on Josephson junctions. The non-linearity of the Josephson junction plays a crucial role in the quantum dynamics of the device. Using monochromatic microwaves, we are able to manipulate up to about ten quantum states coherently.

Specifically, the quantum system that we have studied in our experiments is a current-biased dc SQUID. It consists of two Josephson junctions each with critical current I_0 and capacitance C_0 . The junctions are embedded in a superconducting loop of inductance L_s , threaded by a flux Φ . Since $L_s I_0 \approx \Phi_0/2\pi$, the phase dynamics of the two junctions can be treated as that of a fictitious particle of mass $m = 2C_0(\Phi_0/2\pi)^2$ moving in a two-dimensional potential, which contains valleys and mountains [21, 22, 23]. Here $\Phi_0 = h/2e$ is the superconducting flux quantum. The local minima are separated from each other by saddle points, where the particle can escape. Along the escape direction, the potential is cubic and can be characterized by a frequency ω_p and a barrier height ΔU , see Fig. 1A. These two quantities depend on the magnetic flux and vanish at the critical current I_c of the SQUID. We assume a complete separation of the variables along the escape direction and the transverse one by neglecting the coupling terms between these two directions. In this approximation, the dynamics of the SQUID's phase ϕ along the escape direction is similar to the dynamics of the phase of a current-biased single Josephson junction [24, 25]. The parameters I_c , ΔU and ω_p are renormalized, thereby taking into account the two-dimensional

nature of the potential, as it was demonstrated in [21, 22]. For bias currents I_b below I_c , the particle is trapped in a local minimum and its quantum dynamics is described by

$$\hat{H}_0 = \frac{1}{2}\hbar\omega_p(\hat{P}^2 + \hat{X}^2) - \sigma\hbar\omega_p\hat{X}^3, \quad (1)$$

where $\hat{P} = (1/\sqrt{m\hbar\omega_p})P$ and $\hat{X} = (\sqrt{m\omega_p/\hbar})\phi$ are the reduced momentum and position operators, respectively. Here, P is the operator conjugate to ϕ ; $\sigma = 1/(6a)[2(1 - I_b/I_c)]^{-5/8}$ is the relative magnitude of the cubic term compared to the quadratic (harmonic) term. The parameter a is a constant, $a \sim 11$ for our SQUID. For I_b well below I_c , $\Delta U \gg \hbar\omega_p$ and many low-lying quantum states are found near the local minimum. These states, describing the oscillatory motion within the anharmonic (cubic) potential, are denoted $|n\rangle$ for the n th level, with $n = 0, 1, 2, \dots$. The corresponding energies were calculated in Ref. [25]. The tunnelling through the barrier can be neglected for the lowest-lying states with $n\hbar\omega_p \ll \Delta U$. In our quantum circuit, we manipulate these deep quantum states with a time-dependent flux $\Phi(t)$. Its effect can be included in Eq. (1) by adding the time-dependent term $\alpha(t)\hbar\omega_p\hat{X}$ where $\alpha(t)$ is proportional to $\Phi(t)$ [26].

Our procedure to perform quantum experiments consists of four successive steps as depicted in Fig. 1B. A bias current I_b is switched on through the SQUID at fixed magnetic flux Φ_{dc} to prepare the circuit at the working point in the initial ground state $|0\rangle$. Upon the application of a microwave (MW) flux pulse, this state evolves into a coherent superposition $|\Psi\rangle = a_0|0\rangle + a_1|1\rangle + \dots + a_n|n\rangle + \dots$. Then, a flux pulse of nanosecond duration is applied which brings the system to the measuring point such that the state $|\Psi\rangle$ is projected onto either the zero or the finite voltage state of the SQUID (Fig. 1C). The result of this quantum measurement can be read out by monitoring the voltage V_{out} across the dc SQUID. Finally, I_b is switched off such that the circuit is reset and the experiment can be repeated. Repetitive experiments were performed to obtain state occupancy.

The aforementioned quantum measurement procedure was discussed theoretically by us in Ref. [26]. Differently from previous experiments which used current bias pulses [3, 6] or MW pulses [4], we implemented a quantum measurement using a large-amplitude flux pulse with nanosecond duration. This flux pulse reduces the SQUID critical current to a value very close to the bias current such that $\Delta U \sim \hbar\omega_p$. As a result, the probability to escape from $|0\rangle$ during the pulse is very different from the probability to escape from an excited state. We use a pulse of $2.5ns$ duration whose $1.5ns$ rise and fall times are long enough to

guarantee adiabaticity: transitions between $|0\rangle$ and excited states are estimated to occur with a probability less than 1% for a typical pulse amplitude of $0.06\Phi_0$. The measurement pulse is applied with a variable delay after the end of the MW pulse. This delay is kept as short as $1.5ns$ to limit relaxation processes. Ideally, the pulse projects the excited states with $n > 0$ onto the voltage state (V_{out} is twice the superconducting gap), and the ground state $|0\rangle$ onto the zero-voltage state with an efficiency estimated to be 96% for a one-shot measurement [26]. As the SQUID is hysteretic, the zero and finite voltage states are stable. The result of the quantum measurement is obtained by measuring the escape probability P_{esc} repeating the experiment up to about 4000 times.

The measured dc SQUID consists of two aluminum Josephson junctions with $I_0 = 3.028\mu A$ and $C_0 = 0.76pF$, coupled by an inductance $L_s = 98pH$ (see Fig. 1D). The quantum circuit is decoupled from the external classical circuit by long on-chip superconducting thin wires of large total inductance, $L_e = 15nH$, and a parallel capacitor, $C_e = 150pF$. The quantum circuit and the long superconducting wires are realized by e-beam lithography and shadow evaporation [27]. The nominal room temperature microwave signal is guided by 50Ω coax lines and attenuated twice by 20dB (at 1.5K and 30mK, respectively) before reaching the SQUID through a mutual inductance $M_s = 0.7pH$. The MW line is terminated by an inductance estimated to be $L_{MW} = 1nH$. Special care was taken to avoid spurious environmental microwave resonances. Indeed the chip is mounted in a shielded copper cavity, cooled down to about 30 mK, whose cut-off frequency is above 20 GHz. Moreover, the thin film capacitor, C_e , close to the chip decouples the microwave signal from the low-frequency bias lines.

The escape probability is first obtained by measurements using long (duration $\Delta t = 50\mu s$) pulses of the bias current I_b . From the dependence of the escape current (defined as the current at which $P_{esc} = 1/2$) on Φ_{dc} , the experimental parameters of the SQUID are extracted [21]. At the maximum value of I_c obtained for $\Phi_{dc}/\Phi_0 = -0.085$, the measured escape rate can be fit by the well-known MQT formula [21, 23] yielding the same SQUID parameters within a 2 % error. This result confirms that the circuit remains in the ground state when only I_b pulses are applied. For other values of Φ_{dc} , the width of the escape probability is larger than the MQT prediction by a factor up to 4 indicating a residual low-frequency flux noise in our sample [6]. This noise reduces the efficiency of our quantum measurement since it smoothens the escape probability difference between the ground state

and the excited states. Therefore in our experiment, the maximum efficiency was coarsely estimated at about 30% between $|0\rangle$ and $|1\rangle$.

Spectroscopic measurements were performed by sweeping the frequency of a MW flux pulse of $25ns$ duration in the low power limit. In the inset of Fig. 2 we show the corresponding resonance peak found for P_{esc} versus microwave frequency ν . The resonant frequency ν_{01} depends on I_b as shown in Fig. 2; this dependence can be very well fit by the semiclassical formula for the cubic potential [25]. The parameters extracted from this fit are consistent within 2% error with the parameters extracted from the critical current versus flux dependence or from the MQT measurements at $\Phi_{dc}/\Phi_0 = -0.085$. The large width $\Delta\nu_{01} = 180MHz$ of the resonance peak is consistent with the presence of a residual low-frequency flux noise. Indeed, since the flux through the SQUID fluctuates slowly, the expected resonant frequency changes from one measurement to the other.

We also measured the lifetime of the first excited states, analyzing the decay of the height of the resonance. Upon increasing the delay time between the end of the MW pulse and the nanosecond dc measuring pulse, the peak height is found to decay with times ranging from 14ns to 60ns. The frequency broadening associated with these finite lifetimes is estimated to be smaller than 10MHz, i.e., not only less than the observed width $\Delta\nu_{01}$ of the resonance peak but also less than the detuning frequency associated with the anharmonicity between adjacent levels.

By applying short MW pulses at the resonant frequency $\nu = \nu_{01}$, we induce coherent quantum dynamics. Coherent oscillations were observed by measuring escape probability versus MW pulse duration, as shown in Fig. 3 for three different values of MW power. Oscillation amplitudes as large as 70% were observed for the largest MW power. The oscillations are damped with a characteristic attenuation time of about $12ns$. Similar coherent oscillations have been observed at different working points. The frequency of the coherent oscillations depends on the MW power. This is seen in Fig. 4, where we plot the oscillation frequency as a function of the amplitude Φ_{MW} of the MW pulse. We do not find the linear dependence predicted by Rabi theory for a two level system [28].

To explain the coherent oscillations, we have generalized the Rabi theory to a multi-level anharmonic system described by the Hamiltonian \hat{H}_0 , Eq. (1), whose unperturbed energy levels E_n are given by Ref. [25]. We assume the MW pulse to couple the eigenstates $|n\rangle$ to its nearest-neighbor levels only by the approximate relation $\hat{X}|n\rangle \approx (\sqrt{n+1}|n+1\rangle +$

$\sqrt{n}|n-1\rangle)/\sqrt{2}$. We thus replace the total time-dependent Hamiltonian $\hat{H}_0 + \alpha(t)\hbar\omega\hat{X}$ by the approximate Hamiltonian $\hat{H}_a(t)$,

$$\hat{H}_a(t) = \sum_n E_n |n\rangle\langle n| + \alpha(t)\hbar\omega_p \sum_n \sqrt{n/2} [|n\rangle\langle n-1| + |n-1\rangle\langle n|], \quad (2)$$

where $\alpha(t)$ is the dimensionless amplitude of the classical incident MW field which is proportional to $\Phi_{MW} \cos(2\pi\nu t)$. Here Φ_{MW} is the microwave flux amplitude through the SQUID. Using the rotating wave approximation, we have solved the time-dependent Schrödinger equation $i\hbar\partial|\Psi\rangle/\partial t = \hat{H}_a|\Psi\rangle$, treating the coupling to the microwaves non-perturbatively. Starting with $|\Psi(t=0)\rangle = |0\rangle$ as the initial state, coherent oscillations are predicted involving a number of states in the anharmonic well that increases with increasing microwave amplitude Φ_{MW} . The measured dependence of the frequency of these coherent oscillations as a function of Φ_{MW}/Φ_0 is perfectly fit by the dependence predicted by the model (see Fig.4). The MW power calibration found from the fit is consistent, within a 30 % error, with the actual applied MW amplitude and with the microwave line and coupling parameters, which were measured independently. The coherent oscillation occurs between two extreme states: $|0\rangle$ and a coherent superposition of several quantum states of the anharmonic well. At low power ($\Phi_{MW}/\Phi_0 = 4.10^{-4}$), the oscillation involves mainly the states $|0\rangle$, $|1\rangle$ and $|2\rangle$ and the frequency is very close to the Rabi oscillation frequency of a two-level system. At larger power, transitions to the higher states become important and the oscillation frequency deviates strongly from the linear regime. In our experiment, the MW power is large enough to couple up to about ten levels localized in the cubic potential.

We reported, to the best of our knowledge, the first observation of coherent oscillations in a multi-level solid-state-based integrated circuit. In our experiment, we have induced coherent superpositions of quantum states using monochromatic microwaves. In order to perform the quantum measurement, we implemented a new measurement procedure based on nanosecond flux pulse through the SQUID. The perfect agreement between our results and the theory proves that the essential physics of our non-linear quantum circuit is well understood.

Multi-level quantum systems with non-equidistant levels are of interest for quantum information processing. Large numbers can be stored and retrieved employing the phase of a N -level quantum system [11]. Moreover, an individual multi-level system can be used to efficiently solve datasearch problems using quantum algorithms that do not rely on entan-

glement [10]. The next step towards the implementation of these ideas will be to achieve a control of all the quantum states in our solid state multilevel system, for instance by using microwaves with a discrete frequency spectrum as proposed in [12, 13].

We thank B. Camarota, F. Faure, Ph. Lafarge, L. Lévy, D. Loss, M. Nunez-Regueiro, B. Pannetier, J. Pekola, and A. Ratchov for useful discussions. This work was supported by the ACI and ATIP programs, as well as by the Institut de Physique de la Matière Condensée, Grenoble. FH acknowledges support from Institut Universitaire de France as well as the hospitality of NTT Basic Research Laboratories.

-
- [1] Yu. Makhlin, G. Schön, and A. Shnirman, *Rev. Mod. Phys.* **73**, 357 (2001).
 - [2] Y. Nakamura, Yu. A. Pashkin, and J. S. Tsai, *Nature* **398**, 786 (1999).
 - [3] D. Vion, *et al.*, *Science* **296**, 886 (2002).
 - [4] John M. Martinis, S. Nam, J. Aumentado, and C. Urbina, *Phys. Rev. Lett.* **89**, 117901 (2002).
 - [5] Y. Yu, S. Han, X. Chu, S. I. Chu, and Z. Wang, *Science* **296**, 889 (2002).
 - [6] I. Chiorescu, Y. Nakamura, C.J.P.M. Harmans, and J. E. Mooij, *Science* **299**, 1869 (2003).
 - [7] T. Yamamoto, Yu. A. Pashkin, O. Astafiev, Y. Nakamura, and J. S. Tsai, *Nature* **425**, 941 (2003).
 - [8] T. Hayashi, T. Fujisawa, H. D. Cheong, Y. H. Jeong, and Y. Hirayama, *Phys. Rev. Lett.* **91**, 226804 (2003).
 - [9] R. Hanson, B. Witkamp, L. M. K. Vandersypen, L. H. W. van Beveren, J. M. Elzerman, and L. P. Kouwenhoven *Phys. Rev. Lett.* **91**, 196802 (2003).
 - [10] S. Lloyd, *Phys. Rev. A* **61**, R-010301 (1999).
 - [11] J. Ahn, T. C. Weinacht, and P.H. Bucksbaum, *Science* **287**, 463 (2000).
 - [12] M. N. Leuenberger and D. Loss, *Nature* **410**, 789 (2001).
 - [13] M. N. Leuenberger, D. Loss, M. Poggio, and D. D. Awschalom, *Phys. Rev. Lett.* **89**, 207601 (2002).
 - [14] R. V. Voss and R. A. Webb, *Phys. Rev. Lett.* **47**, 265 (1981).
 - [15] J.M. Martinis, M. H. Devoret, J. Clarke, *Phys. Rev. Lett.* **55**, 1543 (1985).
 - [16] J.R. Friedman, V. Patel, W. Chen, S.K. Tolpygo, and J.E. Lukens, *Nature* **406**, 43 (2000).
 - [17] L. Thomas, F. Lioni, R. Ballou, D. Gatteschi, R. Sessoli, and B. Barbara, *Nature* **383**, 145

- (1996).
- [18] J. R. Friedman, M. P. Sarachik, J. Tejada, and R. Ziolo, Phys. Rev. Lett. **76**, 3830 (1996).
 - [19] C. Sangregorio, T. Ohm, C. Paulsen, R. Sessoli, and D. Gatteschi Phys. Rev. Lett. **78**, 4645 (1997).
 - [20] W. Wernsdorfer and R. Sessoli, Science **284**, 133 (1999).
 - [21] F. Balestro, J. Claudon, J. P. Pekola, and O. Buisson, Phys. Rev. Lett. **91**, 158301 (2003).
 - [22] V. Lefevre-Seguin, E. Turlot, C. Urbina, D. Esteve, and M. H. Devoret, Phys. Rev. B **46**, 5507 (1992).
 - [23] S. Li, Y. Yu, Y. Zhang, W. Qiu, and S. Han, and Z. Wang, Phys. Rev. Lett. **89**, 98301 (2002).
 - [24] J. M. Martinis, M. H. Devoret, and J. Clarke, Phys. Rev. B **35**, 4682 (1987).
 - [25] A. I. Larkin and Y. N. Ovchinnikov , Sov. Phys. JETP **64**, 185 (1987).
 - [26] O. Buisson, F. Balestro, J. P. Pekola, and F. W. J. Hekking, Phys. Rev. Lett. **90**, 238304 (2003).
 - [27] F. Balestro, PhD Thesis, Universite Joseph Fourier, Grenoble, France (2003).
 - [28] I. I Rabi, Phys. Rev. B **51**, 652 (1937).

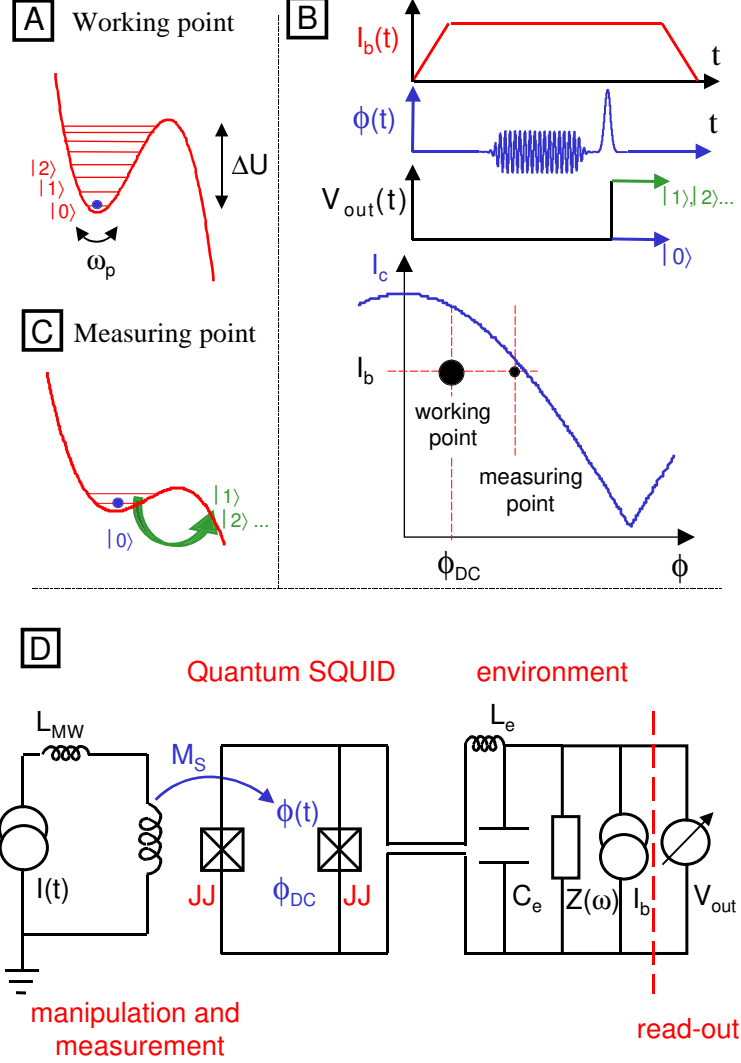


FIG. 1: Manipulation and quantum measurement procedure in a dc SQUID. **(A)** Illustration of the fictitious particle trapped in a deep anharmonic well at the working point. **(B)** Experimental procedure: the current, I_b , is switched on to reach the working point which corresponds to a well of typically 15 levels localized inside with the particle in its ground state. Then, a microwave flux pulse is applied to manipulate the particle inside the well which is followed by a nanosecond flux pulse which carries the system adiabatically from the working point to the measuring point. Finally V_{out} is measured and the current is switched off in order to retrap the particle in a well. **(C)** The well at the measuring point: during the nanosecond flux pulse, the particle can escape or remain in the well depending on its quantum state. **(D)** The dc SQUID consists of two identical Josephson junctions coupled by an inductance L_s . The quantum circuit is decoupled from the environment, symbolized by $Z(\omega)$, by a large inductance L_e and a capacitor C_e ; it is coupled by a mutual inductance M_s to the MW pulse or nanosecond pulse through a 50Ω coax line, terminated by an inductance L_{MW} .

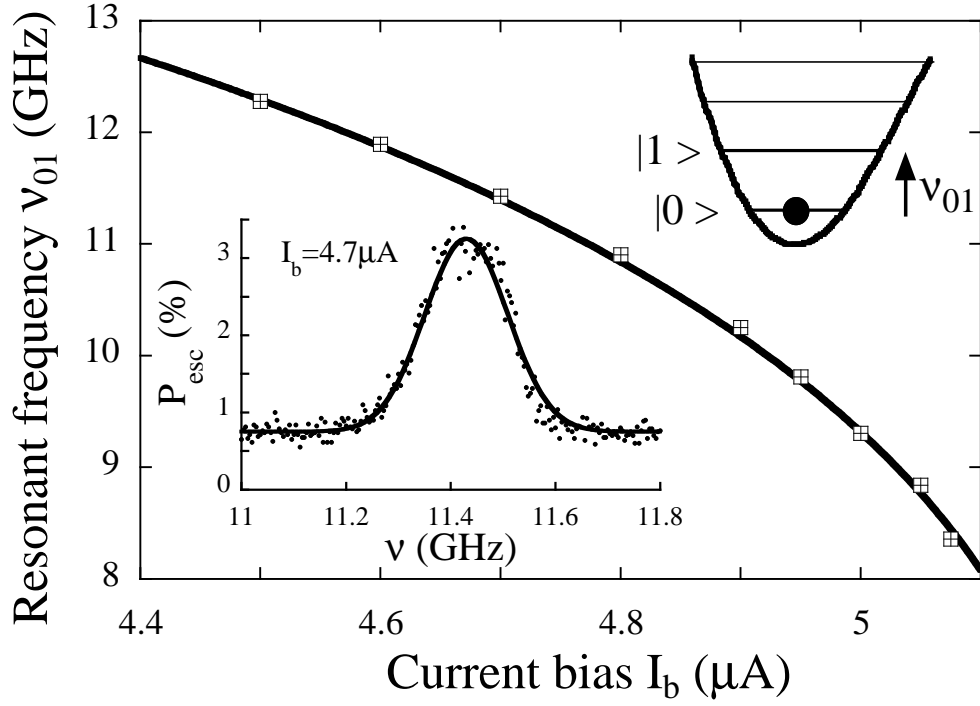


FIG. 2: Resonant transition frequency ν_{01} between states $|0\rangle$ and $|1\rangle$ as function of the bias current at $\Phi_{dc}/\Phi_0 = 0.095$. The experimental dependence of ν_{01} (symbols) on I_b is perfectly described by the semiclassical model [25] (solid line). Spectroscopy is performed by measuring the escape probability P_{esc} versus applied frequency ν (points in inset) at microwave power $A=-48\text{dBm}$ where A is the nominal microwave power at room temperature. The fit to a Gaussian (solid line) defines the resonant frequency $\nu_{01} = 11.43\text{GHz}$ and the width $\Delta\nu_{01} = 180\text{MHz}$.

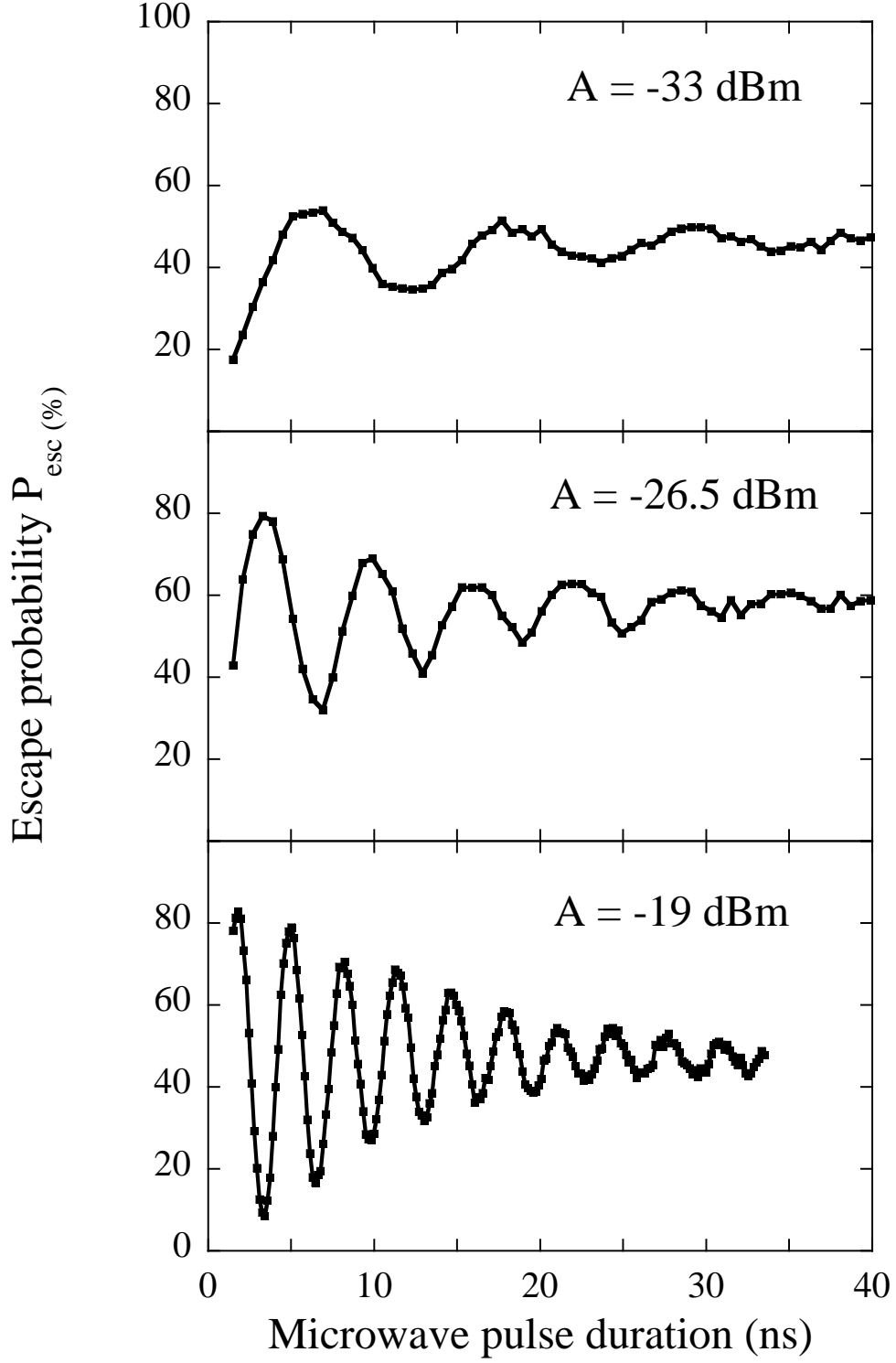


FIG. 3: Coherent oscillations. Measured escape probability versus MW pulse duration for three different MW amplitudes at the working point, defined by $\Phi_{dc}/\Phi_0 = 0.095$ and $I_b = 4.7\mu A$, with about 15 levels localized in the anharmonic well. These coherent oscillations are between the initial state $|0\rangle$ and a coherent superposition involving 3, 5 and 7 states, respectively, for the three MW amplitudes.

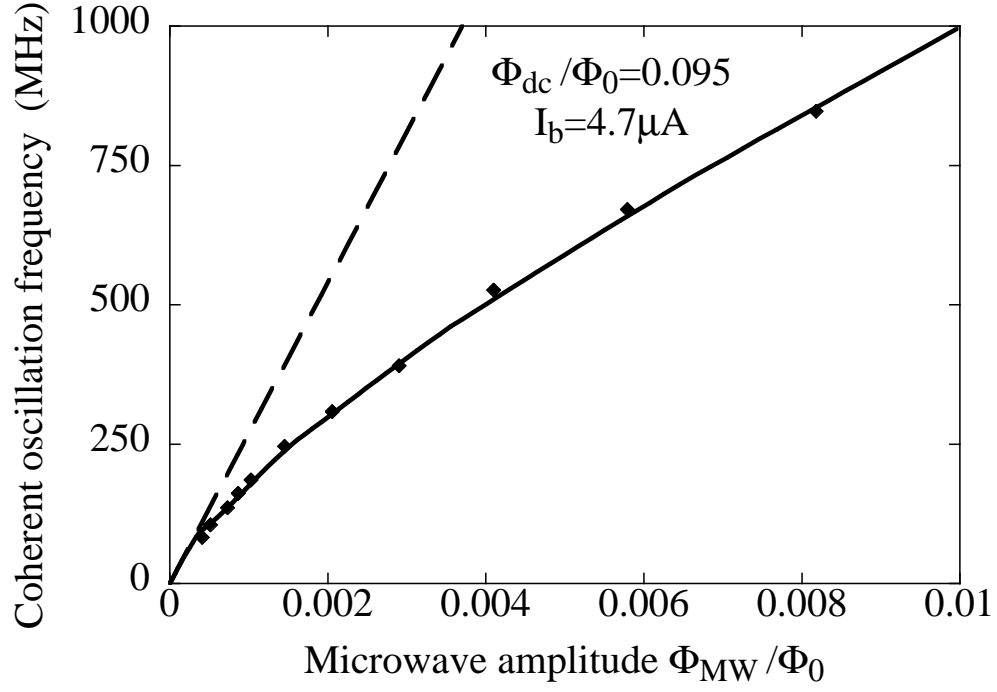


FIG. 4: Frequency of coherent oscillations versus the normalized MW flux amplitude. Dots are experimental results, the solid line the theoretical prediction for a multi-level anharmonic quantum system. Dashed line is the Rabi theory for a two-level system. Experimental calibration of Φ_{MW} is deduced from the fit and is consistent with the estimated Φ_{MW} applied to the set-up.